

Genetic analysis of synaptotagmin 2 in spontaneous and Ca²⁺-triggered neurotransmitter release

Zhiping P Pang¹, Jianyuan Sun¹,
Josep Rizo, Anton Maximov and
Thomas C Südhof*

Departments of Molecular Genetics, Pharmacology, and Biochemistry,
Center for Basic Neuroscience, Howard Hughes Medical Institute, UT
Southwestern Medical Center, Dallas, TX, USA

Synaptotagmin 2 resembles synaptotagmin 1, the Ca²⁺ sensor for fast neurotransmitter release in forebrain synapses, but little is known about synaptotagmin 2 function. Here, we describe a severely ataxic mouse strain that harbors a single, destabilizing amino-acid substitution (I377N) in synaptotagmin 2. In Calyx of Held synapses, this mutation causes a delay and a decrease in Ca²⁺-induced but not in hypertonic sucrose-induced release, suggesting that synaptotagmin 2 mediates Ca²⁺ triggering of evoked release in brainstem synapses. Unexpectedly, we additionally observed in synaptotagmin 2 mutant synapses a dramatic increase in spontaneous release. Synaptotagmin 1-deficient excitatory and inhibitory cortical synapses also displayed a large increase in spontaneous release, demonstrating that this effect was shared among synaptotagmins 1 and 2. Our data suggest that synaptotagmin 1 and 2 perform equivalent functions in the Ca²⁺ triggering of action potential-induced release and in the restriction of spontaneous release, consistent with a general role of synaptotagmins in controlling 'release slots' for synaptic vesicles at the active zone.

The EMBO Journal (2006) 25, 2039–2050. doi:10.1038/sj.emboj.7601103; Published online 27 April 2006

Subject Categories: neuroscience

Keywords: Calyx of Held; neuromuscular junctions; synaptic transmission; synaptotagmin

Introduction

Synaptotagmin 1 is a synaptic vesicle protein that binds Ca²⁺ via its two C₂-domains and functions as a Ca²⁺ sensor for fast neurotransmitter release (Perin *et al*, 1990; Geppert *et al*, 1994; Fernandez *et al*, 2001; Fernandez-Chacon *et al*, 2001). The Ca²⁺ affinities of the synaptotagmin C₂-domains are unphysiologically low (>0.1 mM) in the absence of phospholipids, but are boosted to physiological levels (~1–20 μM

Ca²⁺) in the presence of phospholipids (Ubach *et al*, 1998; Zhang *et al*, 1998; Fernandez *et al*, 2001). In hippocampal synapses and in chromaffin cells, Ca²⁺-binding to synaptotagmin 1 determines the Ca²⁺ affinity of fast exocytosis (Fernandez-Chacon *et al*, 2001; Sorensen *et al*, 2003).

In addition to synaptotagmin 1, 14 other synaptotagmins exist that share the same overall domain structure, but differ in expression patterns and biochemical properties. Among the 'other' synaptotagmins, synaptotagmin 2 most closely resembles synaptotagmin 1 (76% sequence identity in mice), and is the only synaptotagmin besides synaptotagmin 1 that was unequivocally localized to synaptic vesicles (Geppert *et al*, 1991). Synaptotagmins 1 and 2 both bind to SNARE proteins and phospholipids in a Ca²⁺-dependent manner, although with distinct apparent Ca²⁺ affinities (Li *et al*, 1995a,b; Sugita *et al*, 2001, 2002; Rickman *et al*, 2004; Hui *et al*, 2005). These data suggest that synaptotagmins 1 and 2 perform similar functions. Consistent with this hypothesis, synaptotagmin 2 rescues the synaptotagmin 1 deficiency phenotype in neurons and chromaffin cells (Stevens and Sullivan, 2003; Nagy *et al*, 2006). However, synaptotagmin 2 has only been studied in overexpression experiments, and it remains unclear whether synaptotagmins 1 and 2 really perform equivalent functions. One reason for this uncertainty is that although synaptotagmins 1 and 2 share many properties, they also exhibit differences. For example, synaptotagmin 1 is primarily present in the forebrain, which contains almost no synaptotagmin 2, whereas synaptotagmin 2 is more abundant in caudal brain areas (Geppert *et al*, 1991; Ullrich *et al*, 1994; Marqueze *et al*, 1995; Berton *et al*, 1997). Moreover, synaptotagmin 2 but not synaptotagmin 1 selectively binds inositolpolyphosphates (Fukuda *et al*, 1994; Mehrotra *et al*, 2000).

Although synaptotagmin 1 has been studied more extensively than synaptotagmin 2, even its functional definition remains incomplete. Loss-of-function mutants of synaptotagmin 1 cause a decrease in fast Ca²⁺-triggered synchronous release in all preparations tested (Littleton *et al*, 1993; Nonet *et al*, 1993; Geppert *et al*, 1994; Mackler *et al*, 2002; Yoshihara and Littleton, 2002; Sorensen *et al*, 2003; Nishiki and Augustine, 2004), but the additional role of synaptotagmin 1 in other forms of release is unclear. Among others, this is illustrated by results with *Drosophila* synaptotagmin 1 mutants in which an increase of spontaneous release was observed at late larval stages (Littleton *et al*, 1993; Broadie *et al*, 1994; DiAntonio and Schwarz, 1994; Mackler *et al*, 2002), but not at embryonic synapses (Yoshihara and Littleton, 2002), or in larval synapses after acute inactivation of synaptotagmin 1 (Marek and Davis, 2002).

In the present study, we describe mice that contain a point mutation in the synaptotagmin 2 gene. Analysis of synaptic transmission in the Calyx of Held of the mutant mice revealed that Ca²⁺-triggered synchronous neurotransmitter release is decreased, but spontaneous release is enhanced. We show

*Corresponding author. Department of Molecular Genetics, Center for Basic Neuroscience, Howard Hughes Medical Institute, UT Southwestern Medical Center, 6000 Harry Hines Blvd., Dallas, TX 75390-9111 USA. Tel.: +1 214 648 1876; Fax: +1 214 648 1879; E-mail: thomas.sudhof@utsouthwestern.edu

¹These authors contributed equally to this work

Received: 9 January 2006; accepted: 28 March 2006; published online: 27 April 2006

that synaptotagmin 1-deficient cortical neurons also displayed a similar phenotype. Our data, the first functional analysis of synaptotagmin 2 in neurons and of any synaptotagmin in a central synapse *in situ*, reveal that synaptotagmin 1 and 2 generally act in triggering evoked release and in limiting spontaneous release. This result is consistent with the notion that in different types of synapses, synaptotagmin 1 and 2 perform analogous functions in 'release slots' at the active zone (Maximov and Südhof, 2005) where they, possibly in a Ca^{2+} -independent complex with SNARE proteins, simultaneously stabilize primed vesicles in the absence of Ca^{2+} , and trigger the exocytosis of these vesicles in the presence of Ca^{2+} .

Results

An ataxic mouse harboring a point mutation in synaptotagmin 2

Synaptotagmin 2^{I377N} mutant mice were identified in a screen of chemically mutagenized mice by Ingenium Pharmaceuticals, and shown by standard procedures (Russ *et al*, 2002; Stumm *et al*, 2002) to carry a single base pair substitution in exon 8 of the synaptotagmin 2 gene. This base pair change causes a nonconservative substitution (I377N) in the seventh β -strand of the C₂B-domain (Figures 1A and B). Homozygous synaptotagmin 2^{I377N} mutant mice were viable but infertile, weighed less and were severely uncoordinated (Figures 1C and E). On a force actometer (Fowler *et al*, 2001), wild-type (WT) mice walked along the edges of the plate, exploring all four sides with even, smooth movements. In contrast, synaptotagmin 2^{I377N} mutant mice stayed in a small sector of the force plate, and moved abruptly with sudden shifts of the head and tail, often appearing to shoot out of the perimeter of the force plate (Figure 1E). Quantitation of the cumulative movements of mice on the force plate showed that the ataxia index was increased >2-fold in synaptotagmin 2^{I377N} mutant mice compared to littermate WT controls (Figure 1F). Heterozygous mutant mice exhibited no change in weight (Figure 1D) or force-plate behavior (data not shown), indicating that the synaptotagmin 2^{I377N} mutation acts recessively.

As a first test of how the I377N mutation might alter synaptotagmin 2 function, we measured the levels of synaptotagmin 2 and a series of control proteins in the forebrain, cerebellum and spinal cord from littermate WT and synaptotagmin 2^{I377N} mutant mice (Figure 1G and Supplementary Figure S1). Consistent with earlier studies (Ullrich *et al*, 1994; Marqueze *et al*, 1995), synaptotagmin 2 was not detectable in the forebrain, but abundant in caudal brain regions. In the cerebellum and spinal cord from mutant mice, we observed a large decrease in synaptotagmin 2 (to 20–30% of WT levels) but an increase in synaptotagmin 1 (to 130–140% of WT levels; Figure 1G and Supplementary Table 1). No other significant changes were found.

The synaptotagmin 2^{I377N} mutant C₂B-domain is unstable but functional

To test the effect of the synaptotagmin 2^{I377N} substitution on the structural and functional properties of the C₂B-domain, we examined recombinant WT and I377N-mutant C₂B-domains biophysically. The circular dichroism (CD) spectra of WT and mutant C₂B-domains were indistinguishable,

suggesting that the mutant domain folded correctly (Figure 2A). Thermal denaturation curves in the absence or presence of 5 mM Ca^{2+} showed that the mutant C₂B-domain exhibited a sharp melting point that is shifted by Ca^{2+} to higher temperatures, consistent with Ca^{2+} -binding to the properly folded mutant C₂B-domain (Figure 2B). However, both in the absence and presence of Ca^{2+} , the I377N-mutant C₂B-domain was denatured at lower temperatures than the WT C₂B-domain (Figure 2C).

We next investigated whether the I377N mutation alters phospholipid- or SNARE-binding by the C₂B-domain. We measured phospholipid binding with a centrifugation assay that monitors Ca^{2+} -dependent binding of recombinant C₂-domains to liposomes (Fernandez *et al*, 2001), using the double C₂A/B-domain fragment instead of the single C₂B-domain because the properties of the normally occurring double C₂A/B-domain fragment differ from those of the single domains (Earles *et al*, 2001; Fernandez-Chacon *et al*, 2001). To ensure that we did not miss subtle shifts in apparent Ca^{2+} affinity, we included the PKC β C₂-domain as an internal standard (Figure 2D). We found that the apparent Ca^{2+} affinities of WT and mutant C₂-domains were indistinguishable (WT C₂B: $\text{EC}_{50} = 7.0 \pm 0.1 \mu\text{M Ca}^{2+}$; I377N-mutant C₂B: $\text{EC}_{50} = 6.7 \pm 0.1 \mu\text{M Ca}^{2+}$), but higher than that of the PKC C₂-domain ($10.0 \pm 0.0 \mu\text{M Ca}^{2+}$ ($n = 5$)).

We next examined the binding of SNARE proteins to WT and mutant synaptotagmin 2 (Figures 2E and F). We prepared homogenates of the cerebellum and brainstem from WT and synaptotagmin 2^{I377N} mutant mice under conditions favoring SNARE complex assembly, immunoprecipitated synaptotagmin 2 or syntaxin-1 and analyzed the immunoprecipitates by immunoblotting. We found that both WT and I377N-mutant synaptotagmin 2 co-immunoprecipitated with syntaxin-1, SNAP-25 and synaptobrevin-2 (Figures 2E and F). The immunoprecipitations were specific because control antibodies were inactive, and control proteins were not co-immunoprecipitated (data not shown), and because synaptotagmin 1 was not brought down by the synaptotagmin 2 antibodies (Figure 2E). To test whether SNARE proteins bind less well to mutant synaptotagmin 2, or whether binding of synaptotagmin 1 to SNARE proteins is upregulated in mutant synapses, we quantitated the amount of co-immunoprecipitated synaptotagmin 1 and 2 as well as co-immunoprecipitated SNAP-25 and synaptobrevin 2 in syntaxin-1 immunoprecipitates (Figure 2F). However, we found that synaptotagmin 2 mutation did not impair binding of synaptotagmin 2 to immunoprecipitated SNARE complexes, nor did the mutation lead to a compensatory increase in synaptotagmin 1 binding to SNARE complexes. Viewed together, these experiments establish that the synaptotagmin 2^{I377N} mutation impairs the motor behavior of the mutant mice by destabilizing synaptotagmin 2 and depressing synaptotagmin 2 levels without altering the known functional properties of synaptotagmin 2.

Neurotransmitter release in WT and synaptotagmin 2^{I377N} mutant neurons

To measure whether neurotransmitter release is altered in the mutant mice, we examined synaptic transmission in the Calyx of Held synapse, using whole-cell recordings in the MNTB (medial nucleus of the trapezoid body) in acute brainstem slices. Immunofluorescence labeling showed that the Calyx terminals only contain synaptotagmin 2, but no

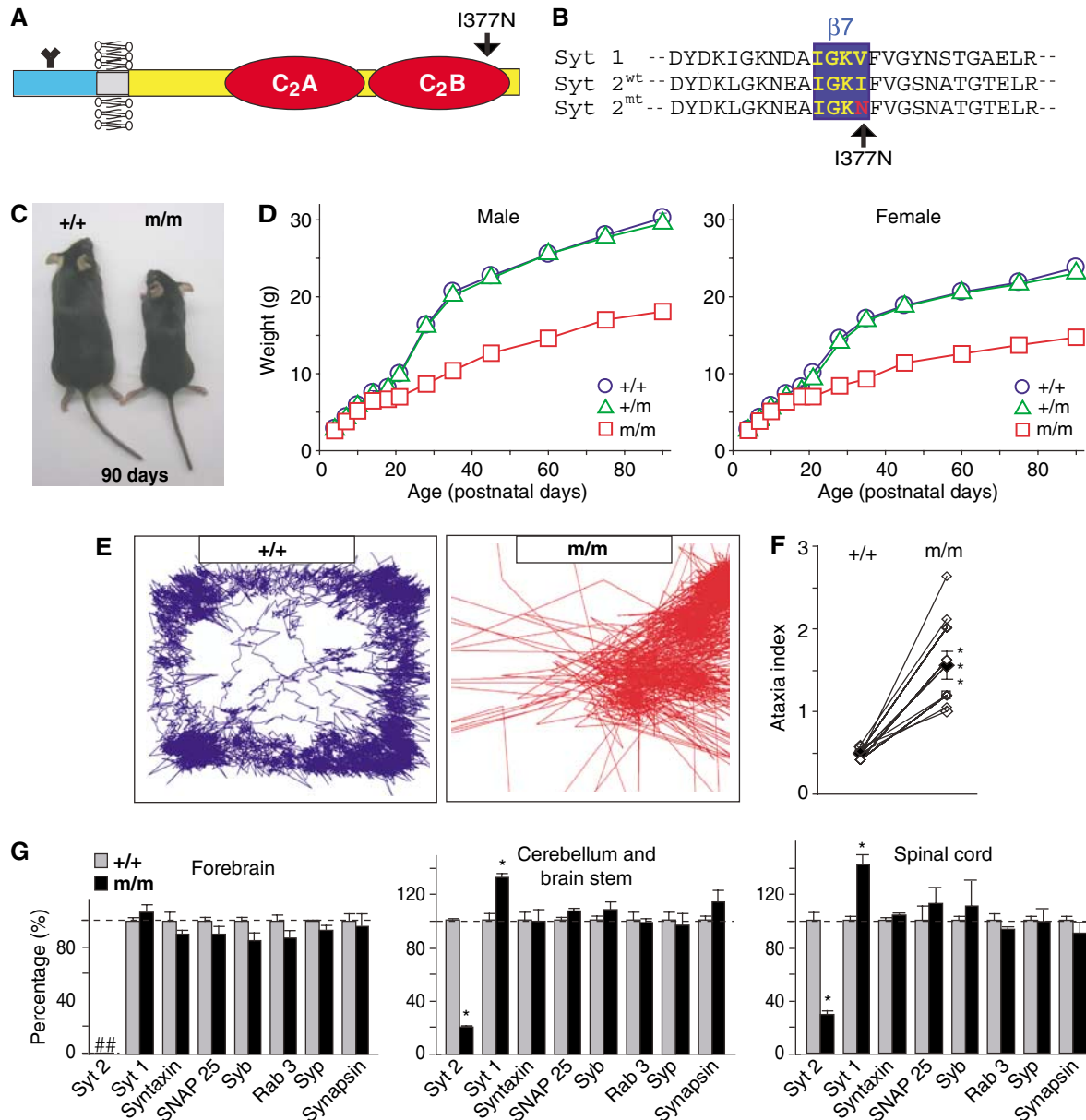


Figure 1 Characterization of synaptotagmin 2^{I377N} mutant mice. (A) Domain structure of synaptotagmin 2; arrow points to position of the I377N substitution. (B) Sequence alignment of WT synaptotagmin 1 and 2 and mutant synaptotagmin 2^{I377N}. (C) Pictures of littermate WT (+ / +) and synaptotagmin 2^{I377N} homozygous mutant mice (m/m). (D) Body weights of WT and hetero- and homozygous mutant male and female mice as a function of age ($n = 10-33$). (E) Representative traces of the movements of littermate WT and synaptotagmin 2^{I377N} mutant mice monitored on a force plate. (F) Ataxia indices of eight independent pairs of littermate WT and synaptotagmin 2^{I377N} mutant mice calculated from force-plate traces ($***P < 0.001$). (G) Protein levels in synaptotagmin 2^{I377N} mutant mice (m/m; black) expressed as the percent of WT levels (+ / +; gray). Protein levels were determined in three independent pairs of littermate WT and synaptotagmin 2^{I377N} mutant mice using quantitative immunoblotting with ¹²⁵I-labeled secondary antibodies and PhosphorImager detection. For additional proteins, see Supplementary data. Abbreviations used: syt 1 and syt 2, synaptotagmin 1 and 2; Syb, synaptobrevin; Syp, synaptophysin ($*P < 0.05$). In these and all subsequent figures, data shown are means \pm s.e.m.'s; statistical significance is assessed with the Student's *t*-test.

detectable synaptotagmin 1 (Figure 3). In synaptotagmin 2^{I377N} mutant Calyx synapses, staining for synaptotagmin 2 is significantly decreased (Figure 3A) as expected from the decrease in synaptotagmin 2 protein levels in the mutant mice (Figure 1), but no upregulation of synaptotagmin 1 was observed (Figure 3B).

We first patched presynaptic Calyx terminals and postsynaptic MNTB neurons simultaneously to monitor both presynaptic Ca²⁺ currents and postsynaptic EPSCs, and stimulated release with a presynaptic depletion protocol

(Sakaba and Neher, 2001). According to this protocol, we depolarized the terminals from -80 to $+80$ mV for 4 ms, partly repolarized them to 0 mV for 50 ms and then returned them to the holding potential of -80 mV (Figure 4A). These experiments were performed with tetrodotoxin (1 μ M), kynurenic acid (1 mM), cyclothiazide (0.1 mM) and D-AP-5 (50 μ M) in the bath solution.

We found that synaptotagmin 2^{I377N} mutant synapses exhibited no major change in presynaptic Ca²⁺ currents (Figure 4A, Supplementary Figure S2), but that the EPSCs

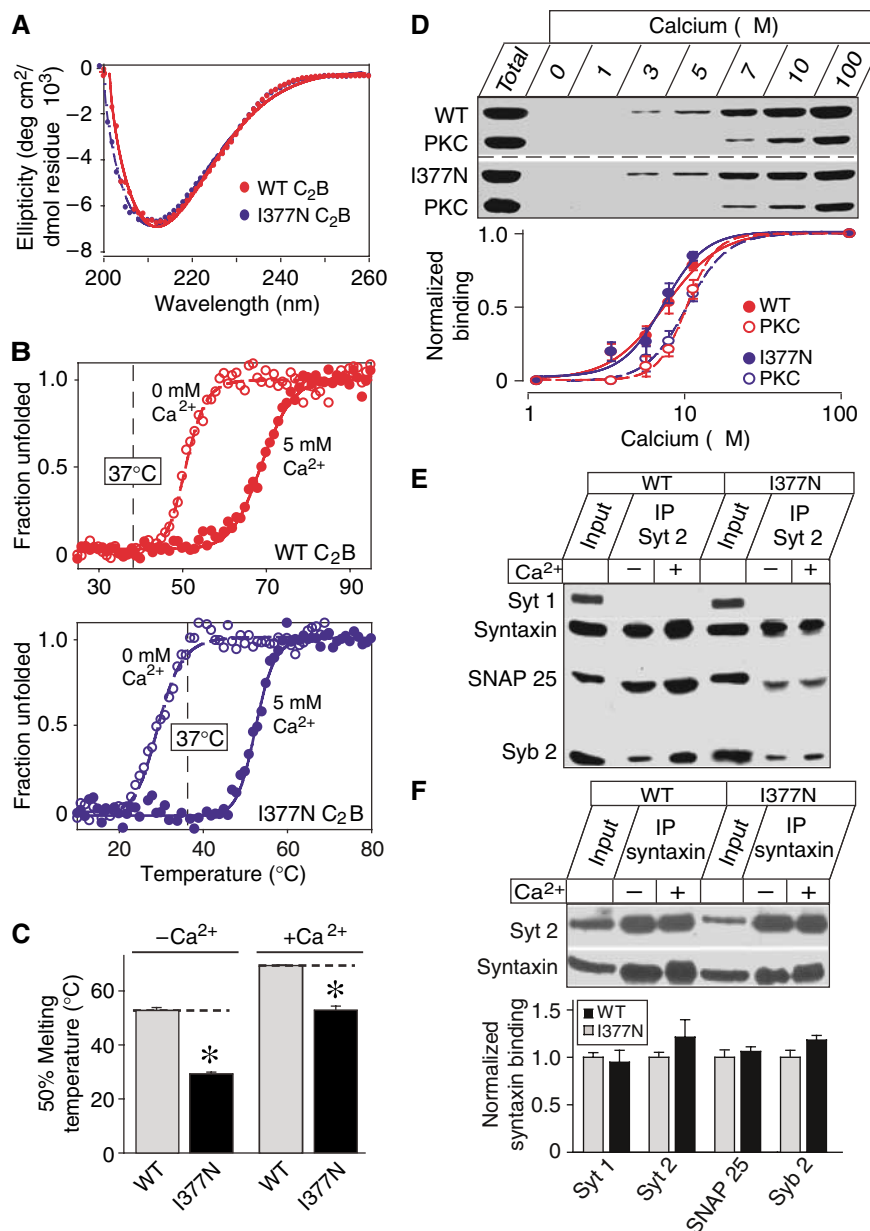


Figure 2 Biochemical characterization of synaptotagmin 2^{I377N} mutant protein. **(A, B)** CD spectra (A) and thermal denaturation curves (B) of WT and I377N-mutant synaptotagmin 2 C₂B domains. Denaturation was monitored by CD at 217 nm without or with 5 mM Ca²⁺. **(C)** Mean 50% melting temperature of WT and I377N-mutant C₂B-domain without or with 5 mM Ca²⁺ (**P* < 0.05). **(D)** Ca²⁺-dependent phospholipid binding by the double C₂AB-domain fragment from WT and I377N-mutant synaptotagmin 2 (tested as purified GST fusion proteins). Liposomes (25% PS/75% PC) were incubated at the indicated free Ca²⁺ concentrations with the C₂AB-domain fragment of synaptotagmin 2 and the C₂-domain of PKCβ (as an internal control); bound C₂-domains were measured by SDS-PAGE and Coomassie staining. Upper panel shows a representative Coomassie-stained gel; binding was quantified in multiple independent experiments by scanning of Coomassie-stained gels as shown in lower panel. **(E, F)** Binding of WT and I377N-mutant synaptotagmin 2 to SNARE complexes analyzed by immunoprecipitations. Synaptotagmin 2 (E) or syntaxin-1 (F) were immunoprecipitated from detergent-solubilized brain extracts from control and synaptotagmin 2^{I377N} mutant mice without or with Ca²⁺; co-precipitated proteins were examined by immunoblotting (syt 1 and 2 = synaptotagmins 1 and 2; Syb 2 = synaptobrevin 2). In (F), the amount of synaptotagmins 1 and 2, SNAP-25 and synaptobrevin 2 present in the syntaxin-1 immunoprecipitates in the absence of Ca²⁺ were quantified using ¹²⁵I-labeled secondary antibodies and PhosphorImager detection.

displayed a significantly longer latency, slower risetimes and decreased EPSC amplitudes, consistent with a role for synaptotagmin 2 in Ca²⁺ triggering of release (Figure 4B–D). The total charge transfer, when integrated over 2 s, was not significantly different between WT and mutant synapses (Figure 4E), whereas the kinetics of release was dramatically altered. Plotting the normalized charge transfer as a function of time and fitting it with a three-exponential function

(Figure 4F) revealed that the time constant for the first component of release was >2-fold longer for mutant than for WT synapses, while the time constants for the second and third components were unchanged (Figure 4G). Moreover, the relative contributions of the three components to total release changed significantly: in WT synapses, the second component accounted for almost 90% of the total charge transfer, whereas in mutant synapses, the contribution of the

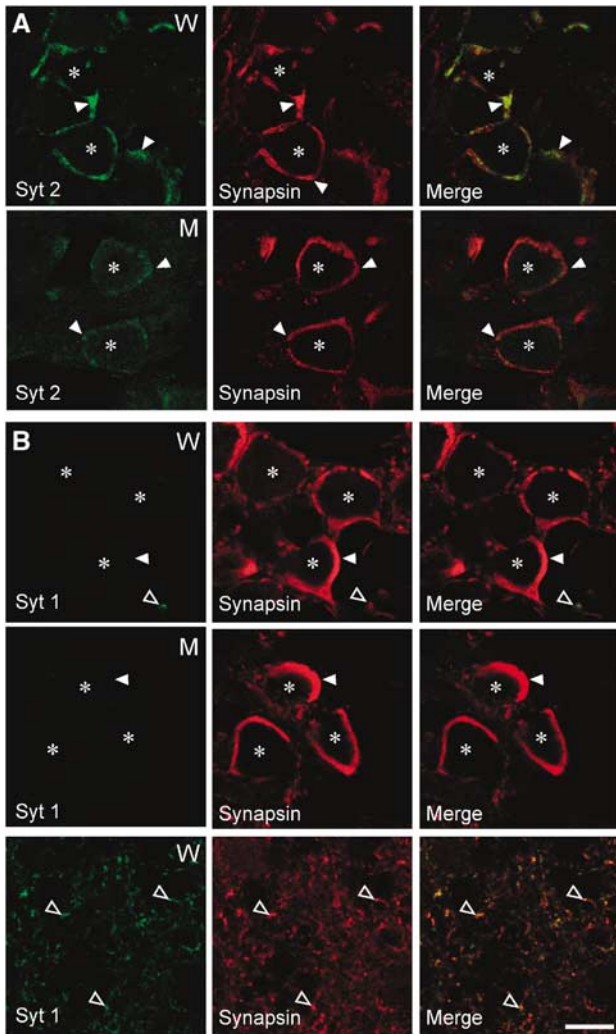


Figure 3 Synaptotagmin 2 but not synaptotagmin 1 is present in Calyx terminals. Panels show double immunofluorescence labeling experiments of brainstem sections from wild-type and synaptotagmin 2^{1377N} mutant mice with antibodies to synaptotagmin 2 (syt 2) and synapsins (A) or to synaptotagmin 1 and synapsins (B). Note that although no synaptotagmin 1 can be detected in wild-type (W) or mutant Calyx terminals (M) in the ventral brainstem, synaptotagmin 1 is abundantly expressed in smaller terminals in the dorsal brainstem (bottom panels in B). Closed arrowheads identify Calyx presynaptic terminals; open arrowheads non-Calyx terminals; * = soma of postsynaptic MNTB neurons. Bar = 10 μ m.

second component was halved, but the contribution of the third component increased five-fold (Figure 4H).

To examine release triggered by action potentials (APs), we induced APs by afferent fiber stimulation, and measured postsynaptic responses by whole-cell recordings. The amplitude and charge of the AP-induced EPSCs were significantly smaller in synaptotagmin 2^{1377N} mutant than in WT synapses (Figures 5A and B). In addition, we unexpectedly found that the frequency of unitary release events was dramatically enhanced in synaptotagmin 2^{1377N} mutant synapses (Figure 5C). In the following discussion, we refer to all unitary release events as 'minis', independent of whether they are recorded from resting synapses or from synapses stimulated by APs. At rest, the miniature EPSC (mEPSC) frequency was potentiated almost five-fold in mutant synapses (Figure 5C). After an AP, the mini frequency was

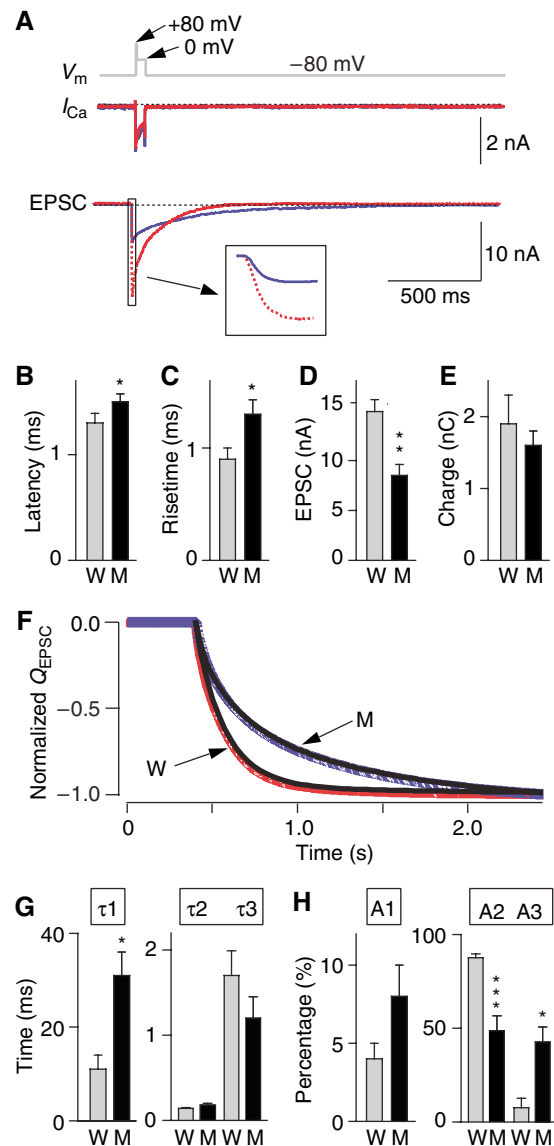


Figure 4 Kinetics of release in Calyx synapses in response to a 50 ms presynaptic depolarization. Simultaneous pre- and postsynaptic voltage-clamp recordings were obtained in brainstem slices from WT and synaptotagmin 2^{1377N} mutant mice at P7-P9 in the presence of 0.1 mM CTZ, 1 mM kynurenic acid and 50 μ M D-AP5. (A) Experimental protocol (top gray line) and representative traces of presynaptic Ca^{2+} currents (I_{Ca}) and postsynaptic EPSCs in WT (W; red) and mutant mice (M; blue). In the bottom panels, representative WT and mutant I_{Ca} and EPSCs traces are superimposed; inset shows an enlargement of the initial phase of the EPSCs. (B-E) Quantitative comparison of EPSCs from WT and synaptotagmin 2^{1377N} mutant synapses: latencies from the onset of the Ca^{2+} current to 10% of the EPSC (B), 20-80% rise times (C), amplitudes (D) and synaptic charge transfer integrated over 2 s (E; W: $n=12$; M: $n=14$ for B-D; W: $n=6$; M: $n=8$ for E). (F) Normalized integrals of EPSC charge transfer over 2 s from littermate WT (W; red) and mutant mice (M; blue). The integration traces are fitted by three-exponential functions (black line, $r^2 > 0.9999$). (G, H) Time constants (G) and fraction (H) of each component from a three-exponential function fitting for each trace of the integral of EPSCs from WT ($n=6$) and synaptotagmin 2 mutants ($n=8$).

increased in both WT and mutant synapses, but the absolute increase was ~ 2 -fold higher in mutant than in WT synapses (Figure 5D). The augmentation in mini frequency in synaptotagmin 2^{1377N} mutant synapses, however, was insufficient

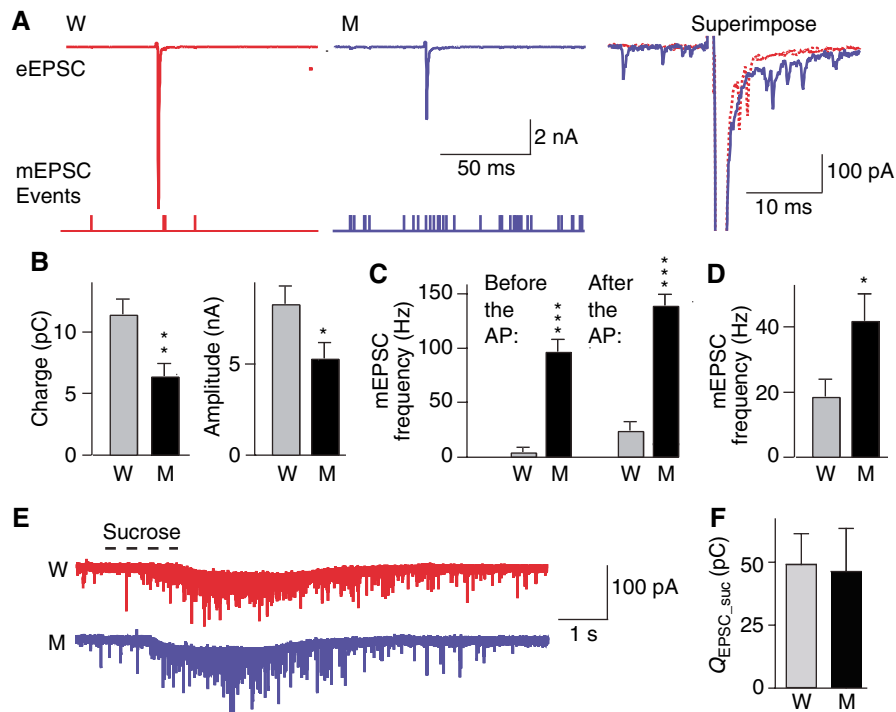


Figure 5 Release evoked by single APs or hypertonic sucrose in Calyx synapses at postnatal day P14. (A) Representative EPSC traces monitored in the presence of bicuculline (10 μ M), strychnine (10 μ M) and D-AP-5 (50 μ M) in response to isolated APs evoked by fiber stimulation (WT = W; red; synaptotagmin 2^{1377N} mutants = M; blue); traces are scaled and superimposed on the right. Below the traces, mEPSC events are indicated as notches. (B) Mean electrical charge transfer (integrated over 100 ms) and amplitude of evoked EPSCs. (C) Frequency of mEPSCs in the 100 ms periods before and after stimulation. (D) Absolute increases in mEPSCs frequency in 100 ms after stimulation (W: $n = 12$; M: $n = 9$). (E) Representative recordings of mEPSCs induced by a 1 s puff of hypertonic sucrose (a glass pipette containing 2 M sucrose positioned $\sim 5 \mu$ m from the Calyx, and puffed the sucrose solution onto the terminal using a 1 s pressure pulse as indicated by the dashed line above the traces) from WT (W; red) and mutant (M; blue). (F) Average charge transfer during hypertonic sucrose-induced mEPSCs from WT ($n = 4$) and mutant ($n = 4$) integrated over 5 s (* $P < 0.05$; ** $P < 0.01$; *** $P < 0.001$).

to compensate for their decrease in synchronous release, because the total charge of the AP-induced EPSC (the sum of synchronous and spontaneous release) when integrated over 100 ms was significantly reduced in synaptotagmin 2^{1377N} mutant synapses (Figure 5B; please note that this result refers to an AP-induced EPSC as opposed to the presynaptic depletion protocol applied in Figure 4E).

The decrease in evoked release and the increase in spontaneous release could reflect abnormal synaptic vesicle priming that establishes the readily releasable pool of vesicles (RRP). One operational definition of the RRP is the amount of release triggered by the application of hypertonic sucrose, which provokes Ca²⁺-independent release of vesicles (Rosenmund and Stevens, 1996). To measure the RRP, we puffed 2 M sucrose onto the terminal for 1 s using a glass pipette that was positioned close to the Calyx (<5 μ m). Hypertonic sucrose induced a train of mEPSCs; integration of the charge transfer revealed that the WT and synaptotagmin 2^{1377N} mutant synapses produced similar amounts of sucrose-induced release (Figures 5E and F).

Release evoked by AP stimulus trains

We next monitored synaptic responses induced by 40 APs applied at 50 Hz, a physiological stimulation frequency for this synapse (Sommer *et al*, 1993). In WT synapses, the EPSC amplitudes initially depressed during the stimulus train to stabilize at a steady-state level, but the EPSC time course remained completely synchronous (Figure 6A). Although the

initial EPSCs were decreased in synaptotagmin 2^{1377N} mutant synapses, no use-dependent depression was observed, and EPSCs stabilized after ~ 5 APs in mutant synapses at the same average amplitude as in WT synapses (Figure 6B). When plotted as normalized data, this behavior manifests as moderate facilitation (Figure 6C). Thus, the increase in residual Ca²⁺ that presumably accumulates during the high-frequency train 'rescues' the decrease in synchronous release in synaptotagmin 2^{1377N} mutant synapses; as a result, the mutant synapses exhibit the same amount of neurotransmitter release as WT synapses after ~ 5 APs (Figure 6B).

As observed in response to a single AP, synaptotagmin 2^{1377N} mutant synapses exhibited a massive stimulation-dependent increase in mini frequency during AP trains (Figure 6D). We plotted the cumulative number of minis as a function of time during the stimulus train, and corrected for the increase in mini frequency in mutant synapses by adjusting the slope of cumulative mini events before stimulation to zero (Figure 6E). The corrected plot thus represents the accumulated mini release during and after the stimulus train. According to the slope of the accumulative mini release, the average rate of mini release during stimulation (indicated by the horizontal bar in Figures 6D and E) was estimated as 0.45 vesicle/ms for synaptotagmin 2 mutant synapses and 0.06 vesicle/ms for WT synapses. In synaptotagmin 2 mutant synapses, the latter part of the trace (after 2.8 s) could be fitted with a double-exponential function ($\tau_1 = 0.21$ s (37%), $\tau_2 = 1.79$ s (63%); Figure 6E). In contrast, the WT trace could

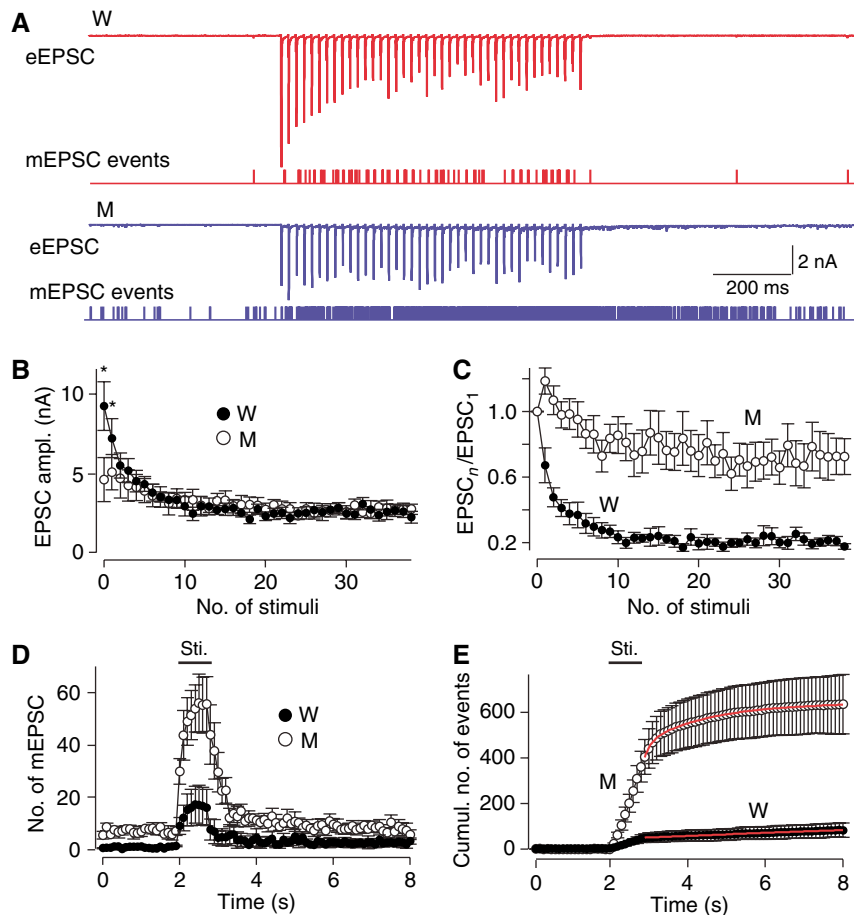


Figure 6 EPSCs evoked by a 50 Hz AP train. (A) Representative traces of EPSCs evoked by 40 APs at 50 Hz (WT, red; synaptotagmin 2^{1377N} mutant, blue). Below the traces, mini events are indicated as notches. (B, C) Absolute (B) and normalized (C) EPSC amplitudes of 40 stimuli at 50 Hz. (D, E) Mini event frequency before, during and after the 50 Hz stimulus train plotted as a function of time as the number of events per 0.1 s interval (D) or as the cumulative number of events after normalization for basal mini release (E; see text for detail). The time of stimulation is indicated by the horizontal bar above the plot (WT, W: *n* = 6, filled symbols; synaptotagmin 2^{1377N} mutant, M: *n* = 5, open symbols).

only be fitted by a single-exponential function with a long time constant (33 s), implying the negligible amount of mini release after stimulation.

Spontaneous neurotransmitter release in WT and synaptotagmin 2^{1377N} mutant neurons

To test whether the increase in mini frequency in synaptotagmin 2^{1377N} mutant synapses reflects an intrinsic alteration of the release machinery or is due to residual bulk Ca²⁺ remaining after an AP, we systematically examined spontaneous minis in MNTB neurons at rest, both from P7–P9 and from P14 mice, and both in the presence or absence of Ca²⁺ (Figure 7). We found that at P7–P9 and at P14, the resting mini frequency was dramatically increased in synaptotagmin 2^{1377N} mutant synapses (>6 times at P7–P9; >12 times at P14), whereas the mini amplitudes and rise times were unchanged (Figure 7). Removal of Ca²⁺ by application of 0.1 mM BAPTA-AM in a Ca²⁺-free bath solution had no effect on the amplitudes and risetimes of minis, but reduced the frequency of minis in both WT and mutant synapses ~10-fold (Figure 7B and D). Even under Ca²⁺-free condition, synaptotagmin 2^{1377N} mutant synapses exhibited an increased mini frequency (~3 times at P7–P9; ~5 times at P14). Quantitatively, Ca²⁺ removal caused a relatively larger

decrease in mini frequency in mutant synapses (~18-fold at P7–P9, ~12-fold at P14) than in WT synapses (~5-fold at both P7–P9 and at P14), indicating that although the mini frequency in mutant synapses is enhanced in the absence of Ca²⁺, it is increased more strongly than in WT synapses by the low levels of Ca²⁺ present in resting synapses.

To ensure that the changes observed are not specific to the Calyx synapse, we additionally monitored minis as miniature endplate potentials (mEPPs) in neuromuscular junctions (NMJs) of diaphragm muscle in WT and synaptotagmin 2^{1377N} mutant mice at P16. Again, we detected a massive increase in mini frequency in mutant synapses (Figure 8A), but no changes of mini amplitudes and risetimes. Next, to confirm the generality of the observed effect of Ca²⁺ on spontaneous release in the Calyx (Figure 7), we tested the effect of Ca²⁺ on mini frequency in NMJs by recording mEPPs either in Ca²⁺-free external solution with BAPTA-AM (to ensure that the conditions are totally Ca²⁺ free) or in external solutions containing 2, 5 or 10 mM Ca²⁺ (Figure 8C). These recordings were performed at P22 when NMJ development is more mature. As in the Calyx synapse, significant spontaneous release was observed even in the total absence of Ca²⁺, but was dramatically enhanced with increasing concentrations of Ca²⁺. At all Ca²⁺ concentrations exam-

ined—both in the complete absence of Ca^{2+} and in the presence of high extracellular Ca^{2+} concentrations—the frequency of mEPPs was several fold higher in mutant NMJs than in NMJs from littermate control mice (Figure 8D).

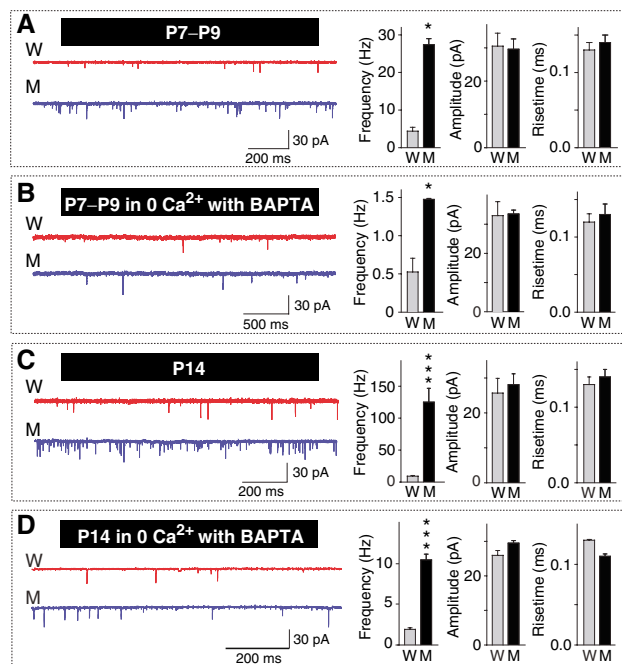


Figure 7 Spontaneous neurotransmitter release in WT and synaptotagmin 2^{I377N} mutant neurons. In all panels, representative traces are shown on the left, and summary diagrams for the mini frequency, amplitude and risetimes (20–80% for the calyx; 10–90% for NMJ) on the right. (A, B) Recordings from the calyx at P7–P9 in regular extracellular medium (A; W: *n* = 7; M: *n* = 8) or medium containing 0 mM Ca^{2+} and 0.1 mM BAPTA-AM (B; W and M: *n* = 6 for both). (C, D) Recordings from the calyx at P14 in regular extracellular medium (C; W: *n* = 8; M: *n* = 9) or medium containing 0 mM Ca^{2+} and 0.1 mM BAPTA/AM (B; W and M: *n* = 9 and 6, respectively) (**P* < 0.05; ****P* < 0.001).

Deletion of synaptotagmin 1 also increases mini frequency

The properties we describe here for synaptotagmin 2^{I377N} mutant synapses resemble those of the synaptotagmin 1-deficient synapses in mice with one exception: no increase in mini frequency was detected in autapses from such mice (Geppert *et al*, 1994; Nishiki and Augustine, 2004), although recent analyses of cortical inhibitory synapses from synaptotagmin 1-deficient mice suggested that such an increase may in fact occur (Maximov and Südhof, 2005). To examine this question, we measured the mini frequency in synapses formed by cultured cortical neurons from synaptotagmin 1-deficient mice. We monitored both excitatory and inhibitory synapses, and examined the effects of either lowering or raising the Ca^{2+} concentration (Figures 9A–D). In resting excitatory and inhibitory synapses, deletion of synaptotagmin 1 enhanced the mini frequency ~5-fold. Decreasing Ca^{2+} in the bath depressed, whereas increasing Ca^{2+} augmented the mini frequency both in WT and mutant synapses; however, under both conditions the large difference between the mutant and WT synapses was retained (Figure 9D). The addition of EGTA-AM to remove intracellular Ca^{2+} had little further effect on mini frequency in WT and mutant synapses. Thus, synaptotagmin 1-deficient cortical synapses behave very similar to synaptotagmin 2^{I377N} mutant synapses in that an intrinsic difference in mini frequency is present. In synaptotagmin 1-deficient synapses, this difference is not a compensatory change in response to the decrease in release because it persisted even after prolonged treatment of the cultures with TTX, which should abolish all network activity in WT and mutant synapses (Figure 9D).

We next applied two closely spaced APs to examine whether stimulation of release increases mini frequency in synaptotagmin 1-deficient neurons. We found that after the APs, the mini frequency was enhanced in both WT and mutant synapses, again with mutant synapses exhibiting a higher frequency (Figures 9E and F). The stimulation-dependen-

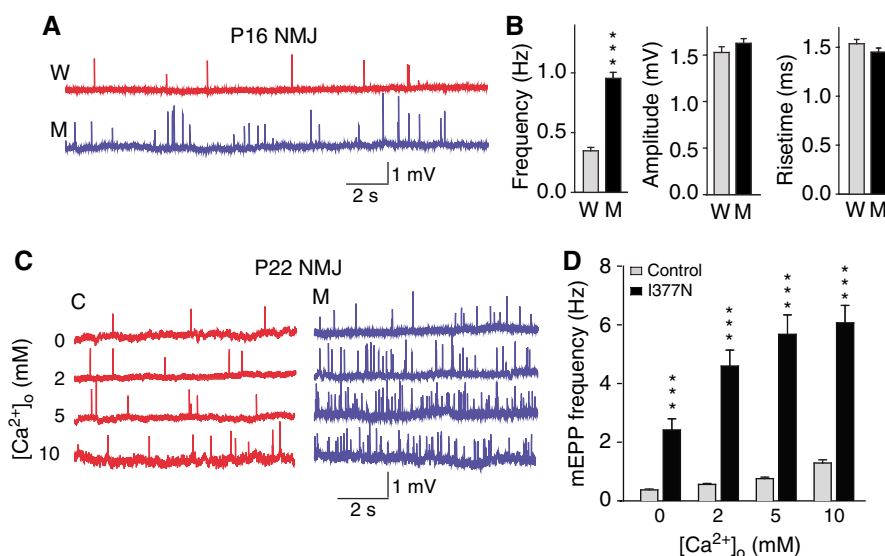


Figure 8 Spontaneous neurotransmitter release at the NMJ. (A, B) Representative traces of mEPPs (A) and summary diagrams of mEPP frequency, amplitude and 10–90% risetimes (B) in diaphragm NMJs from wild-type (W) and synaptotagmin 2^{I377N} mutant mice at P16, recorded in normal Ringer’s solution (W: *n* = 57, three mice; M: *n* = 68, three mice). (C, D) Representative traces of mEPPs (C) and summary diagrams of the mEPP frequencies (D) recorded at the indicated Ca^{2+} concentrations in NMJs from control (C) and synaptotagmin 2^{I377N} mutant mice (M) at P22. Note that the 0 Ca^{2+} condition included BAPTA-AM to remove nerve terminal Ca^{2+} (*n* = 25–30, two animals each genotype) (****P* < 0.001 in B and D).

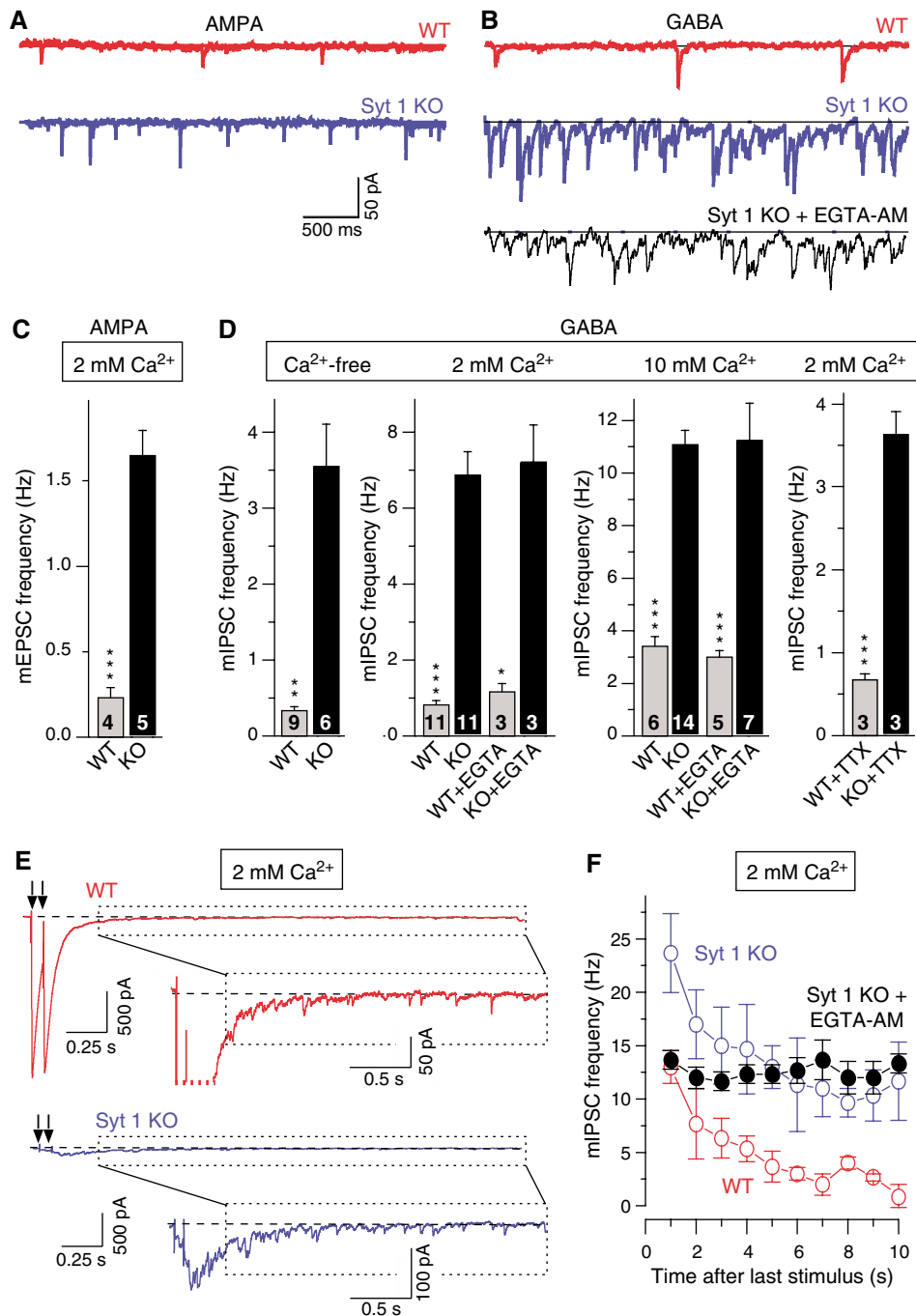


Figure 9 Spontaneous release in synaptotagmin 1-deficient cortical neurons. (A, B) Representative spontaneous mEPSCs (A) and mIPSCs (B) recorded in the presence of acutely added TTX (1 μ M) from WT (red) and synaptotagmin 1-deficient neurons (blue). In (B), mIPSCs were also recorded from synaptotagmin 1-deficient neurons preincubated for 5 min in 0.1 mM EGTA-AM (black; holding potential = -70 mV; scale bars apply to all traces). (C, D) Average mEPSC (C) and mIPSC (D) frequencies in WT and synaptotagmin 1-deficient neurons. Extracellular Ca²⁺ concentrations are indicated on the top; number of cells analyzed are shown in the bars. The 2 and 10 mM Ca²⁺ experiments were also carried out after a 5 min preincubation of neurons in 0.1 mM EGTA-AM. The 2 mM Ca²⁺ data on the right were obtained in neurons that were incubated with 1 μ M TTX for 4 days prior to the recordings. (E) Representative IPSCs evoked by two closely spaced (0.1 s interval) APs in the presence of AP5 and CNQX. Insets illustrate individual mini events observed at the ends of evoked responses. (F) Plot of the average mIPSC frequency in WT and synaptotagmin 1-deficient neurons after the neurons were stimulated by two APs separated by 0.1 s. Frequencies were calculated in 1 s bins starting 0.5 s after the second AP in the train. Data are from three different WT, synaptotagmin 1-deficient neurons and synaptotagmin 1-deficient neurons preincubated with 0.1 mM EGTA-AM (* P <0.05; ** P <0.01; *** P <0.001).

dent increase in mini frequency in mutant synapses was abolished by EGTA-AM, demonstrating that it is due to the increase in intracellular Ca²⁺ produced by the APs (Figure 9F).

Discussion

Using mutant mice that carry a single amino-acid substitution (I377N) in synaptotagmin 2, we demonstrate that synapto-

tagmin 2 is an essential component of the Ca^{2+} -triggering machinery for release in the Calyx of Held synapse. Moreover, we show that impairment of synaptotagmin 2 enhances the rate of spontaneous synaptic vesicle exocytosis, as does deletion of synaptotagmin 1. Our study demonstrates that the normal function of synaptotagmin 2 is analogous to that of synaptotagmin 1, although performed in different neurons, thereby extending the synaptotagmin 1 paradigm to synaptotagmin 2. In addition, our data reveal that synaptotagmin 1 and 2 generally limit spontaneous release at a synapse. These results show that synaptotagmin 1 and 2, as integral components of the release machinery, control initiation of fusion pore opening of synaptic vesicles at the active zone.

Effect of the I377N substitution on synaptotagmin 2

Three observations show that the I377N mutation does not change known functional properties of synaptotagmin 2, but destabilizes synaptotagmin 2 in the brain. First, the I377N-mutant C_2B -domain was normally folded (Figure 2A) but exhibited decreased thermal stability (Figures 2B and C). Second, mutant synaptotagmin-2^{I377N} exhibited apparently normal Ca^{2+} -dependent phospholipid binding and Ca^{2+} -dependent and Ca^{2+} -independent SNARE binding (Figures 2D–F). Finally, the levels of mutant synaptotagmin 2^{I377N} were selectively decreased ~5-fold in the brainstem and spinal cord of the mutant mice (Figure 1G). Hence, the phenotypes observed in the I377N-mutant mice likely arise from a reduction in the amount of synaptotagmin 2 protein.

Synaptotagmin 2 functions in the fast Ca^{2+} triggering of neurotransmitter release

In Calyx synapses, the synaptotagmin 2^{I377N} mutation slowed the time course of release and decreased the EPSC amplitude (Figures 4 and 5). Both the latency and risetime of EPSCs were increased (Figures 4B and C). The size of the RRP, as defined by the amount of release that can be triggered with hypertonic sucrose, was unchanged (Figures 5E and F). Overall, this phenotype resembles that of the synaptotagmin 1 deletion in hippocampal (Geppert *et al*, 1994) and cortical synapses (Maximov and Südhof, 2005), suggesting that synaptotagmin 1 and 2 perform analogous functions, although in different synapses.

The I377N mutation impairs release in the Calyx synapse less severely than the synaptotagmin 1 deletion in hippocampal or cortical synapses (Geppert *et al*, 1994; Maximov and Südhof, 2005). This difference is most likely due to the fact that the I377N mutation does not delete synaptotagmin 2, but only decreases its levels (Figure 1, Supplementary Figure S1 and Supplementary Table 1). Thus, residual synaptotagmin 2 may mediate the remaining Ca^{2+} -triggered fast release.

Synaptotagmin function in asynchronous release

Synaptotagmin 1-deficient synapses exhibit no significant change in asynchronous release in response to single APs, but display a selective increase in asynchronous delayed release triggered by trains of APs (Maximov and Südhof, 2005). The delay in the EPSC time course after a 50ms depolarization in synaptotagmin 2^{I377N} mutant synapses suggests that a similar increase in asynchronous delayed release may be present in the synaptotagmin 2 mutant (Figure 4H).

Alternative explanations for this delay are that it is caused by a change in the properties of postsynaptic receptors, such that the receptors remain active longer, or by a decrease in the clearance of glutamate from the synaptic cleft, such that 'lingering' glutamate continues to activate receptors. The fact that the shape of spontaneous minis and of EPSCs triggered by isolated APs is not altered in synaptotagmin 2^{I377N} mutant neurons makes the two alternative explanations implausible. Moreover, it is difficult to imagine a postsynaptic mechanism for synaptotagmin 2 because synaptotagmin 2 is highly enriched in presynaptic vesicles. This indicates that, as previously demonstrated for synaptotagmin 1 mutants (Maximov and Südhof, 2005), the synaptotagmin 2 mutants may exhibit an increase in delayed release.

Synaptotagmin 1 and 2 function in spontaneous 'mini' release

In synaptotagmin 2^{I377N} mutant mice, Calyx and NMJ synapses exhibited large increases in mini frequency at rest, after removal of Ca^{2+} , and after stimulation by APs (Figures 5–8). Thus, the synaptotagmin 2 mutation increases both spontaneous Ca^{2+} -independent fusion and fusion induced by residual Ca^{2+} after an AP. The increase in spontaneous fusion is not a peculiar effect of the I377N mutation, but reflects a general participation of synaptotagmins in spontaneous exocytosis because we observed a comparable increase in mini frequency in both excitatory and inhibitory synapses in cortical neurons from synaptotagmin 1-deficient mice (Figure 9). This increase again was Ca^{2+} -independent, and was not due to a homeostatic effect because the difference was retained after chronic treatment with TTX. Furthermore, in synaptotagmin 1-deficient cortical neurons, minis were also increased after AP stimulation (Figures 9E and F).

Previous studies obtained conflicting data on minis in synaptotagmin mutants. In autapses formed by cultured hippocampal neurons, deletion of synaptotagmin 1 consistently does not increase spontaneous release (e.g., see Geppert *et al*, 1994; Shin *et al*, 2003; Nishiki and Augustine, 2004). However, in the NMJ of *Drosophila*, deletion of synaptotagmin 1 increased mini frequency at least under certain conditions (Littleton *et al*, 1993; Broadie *et al*, 1994; DiAntonio and Schwarz, 1994, see discussion in the Introduction), and overexpression of synaptotagmin 1 or 2 in frog NMJs inhibited spontaneous release (Morimoto *et al*, 1998). We observed an increase in mini frequency for mutations in two different synaptotagmins (synaptotagmin 1 and 2) and four different synapses (the Calyx of Held synapse, the NMJ, and excitatory and inhibitory cortical synapses), suggesting that the lack of this phenotype in autapses is peculiar to that system, and that synaptotagmin 1 and 2 mutations truly alter spontaneous fusion. Moreover, in cultured neurons this phenotype was not abolished by activity blockade (Figure 9D), demonstrating that the mini frequency increase is not a secondary phenomenon of decreased synaptic activity.

Implications for the mechanism of Ca^{2+} triggering of fast release by synaptotagmin 1 and 2

Together with earlier data, our results demonstrate that synaptotagmin 1 and 2 are not passive inhibitors of fusion

that block a constitutive fusion reaction because the total amount of Ca^{2+} -dependent fusion is dramatically decreased in the absence of synaptotagmins. Conversely, synaptotagmin 1 and 2 do not simply act separately from the fusion machinery but are intrinsic components of this machinery because in their absence, spontaneous fusion, even under totally Ca^{2+} -free conditions, is enhanced. Previous observations showed that synaptotagmin 1 is unlikely to be a component of the fusion pore (Sorensen *et al*, 2003). Consistent with these observations, we thus propose that synaptotagmin 1 and 2 bind to assembled SNARE complexes during priming (Shin *et al*, 2003; Rickman *et al*, 2004) to achieve two effects: first, to inhibit spontaneous fusion and evoked fusion triggered by low Ca^{2+} concentrations that are unable to activate synaptotagmin 1 and 2, and second, to position synaptotagmin 1 and 2 close to where the fusion pore will form, presumably by SNARE proteins. This model suggests Ca^{2+} flowing into the terminal during an AP triggers fusion pore opening by binding to the synaptotagmin C_2 -domains, which in turn causes these C_2 -domains to bind to the phospholipid membrane, thereby inducing a mechanical stress on the membrane that is instrumental in catalyzing fusion pore opening.

Although this hypothesis accounts for all currently available data, it raises questions that need to be addressed before it can be considered plausible. A key question relates to SNARE binding: if Ca^{2+} -independent binding of SNAREs by synaptotagmin 1 and 2 is crucial, why do synaptotagmins additionally bind to SNAREs in a Ca^{2+} -dependent manner? Another question regards the role of complexins that bind to SNARE complexes and are essential for normal Ca^{2+} triggering of release, but whose action is obscure (McMahon *et al*, 1995; Reim *et al*, 2001). A third question concerns the nature of asynchronous release during and after APs. Clearly, additional Ca^{2+} sensors must exist, but do these trigger release analogous to, but slower than synaptotagmin 1 and 2, or do these Ca^{2+} sensors simply act indirectly by accelerating reactions upstream of the final fusion step? Future experiments using additional tools that need to be developed will have to address these issues.

Materials and methods

Generation, breeding and analysis of synaptotagmin 2^{I377N} mutant mice

Synaptotagmin 2^{I377N} mutant mice were generated by Ingenium Pharmaceuticals in a screen of chemically mutagenized mice (Russ *et al*, 2002; Stumm *et al*, 2002). All analyses described were performed on littermate offspring of heterozygous matings to control for background effects.

Behavioral assays

Force-plate actometry (Fowler *et al*, 2001) was performed with 3-month-old mice on a force plate (28 cm × 28 cm) for 6 min. The ataxia index was calculated from the area:distance ratio measured from the movement traces monitored over 6 min (normal range: 0.26–0.60).

Expression and purification of recombinant proteins

WT and I377N-mutant synaptotagmin 2 and PKC C_2 -domain expression vectors in pGEX-KG were described previously (Guan and Dixon, 1991; Sugita *et al*, 2001) or generated by mutagenesis. Recombinant C_2 -domain proteins were stripped of their bacterial

contaminants by treatment with benzonase and extensive washing as described (Ubach *et al*, 2001; see Supplementary data).

Centrifugation phospholipid binding assays

Ca^{2+} -dependent phospholipid binding assays were carried out with purified soluble GST fusion proteins in 50 mM HEPES–NaOH, pH 6.8, 0.1 M NaCl and 4 mM Na₂EGTA using a centrifugation assay (Fernandez *et al*, 2001; Shin *et al*, 2002, 2003).

CD spectra

CD spectra were recorded on an Aviv model 62 DS spectropolarimeter at 200 to 260 nm using a 1 mm path-length cell. Thermal denaturation curves were collected by monitoring the absorption at 217 nm, with or without 5 mM Ca^{2+} . The fraction of unfolded protein at each temperature was calculated by using the formula $(I_{\text{obs}} - I_f) / (I_u - I_f)$, where I_{obs} is the observed signal intensity, and I_u and I_f are the signal intensities of the unfolded and folded states, respectively. I_u and I_f as a function of temperature were calculated by extrapolation of the linear regions at the extremes of the unfolding curves.

Immunoprecipitations were performed from brain homogenates using synaptotagmin 2 polyclonal (A320) or syntaxin monoclonal (HPC-1) antibodies essentially as described (Shin *et al*, 2003).

Immunofluorescence labeling of brainstem cryostat sections was performed with antibodies to synaptotagmins 1 or 2 and synapsins (syt 1: 41.1, 1:5000; syt 2: A320, 1:500; synapsin: Cl10.22, 1:1000 or E028, 1:1000) essentially as described (Ullrich *et al*, 1994, see Supplementary data).

Brain slicing and whole-cell recordings from MNTB neurons

Preparation of slices (200 μm thickness), simultaneous whole-cell recordings of the nerve terminal and the postsynaptic neuron were performed mostly as described (Borst *et al*, 1995; Wu and Borst, 1999). Presynaptic whole-cell recordings were made with an EPC-9 amplifier (HEKA, Lambrecht, Germany) and postsynaptic recordings with an Axopatch 200B amplifier (Axon Instruments Inc., Foster City, CA). The pre- and postsynaptic series resistances (<15 MΩ) were compensated by 60 and 98% (lag 10 μs), respectively. Both pre- and postsynaptic currents were low-pass filtered at 5 kHz and digitized at 20 kHz. mEPSCs were analyzed by a home-made program in Igor, which automatically recognizes individual single mini events in the trace.

NMJ recordings

Intracellular recordings from isolated whole diaphragm were made using an Axoclamp 2B amplifier in normal Ringer's solution (for Figure 8A: 136.8 mM NaCl, 5 mM KCl, 1 mM MgCl₂, 1 mM NaH₂PO₄, 12 mM NaHCO₃, 11 mM D-glucose and 2 mM CaCl₂) or in HEPES buffer for the Ca^{2+} titrations (Figure 8B: 140 mM NaCl, 5 mM KCl, 1 mM MgCl₂, 10 mM HEPES, 10 mM glucose, pH 7.4) with a sharp electrode containing 3 M KCl. mEPPs were analyzed by minianalysis software (Synaptosoft Inc., NJ).

Neuronal cortical cultures from E18 or P1 pups of WT or synaptotagmin 1-deficient mice were obtained and used for recordings as described (Maximov and Südhof, 2005).

Statistical analysis

All data are presented as means ± s.e.m.'s, and were analyzed using the two-tailed paired Student's *t*-test.

Supplementary data

Supplementary data are available at *The EMBO Journal* Online.

Acknowledgements

We thank Armin Bareiss, Dr Gabi Stumm and Michael Ade (Ingenium Pharmaceuticals) for the generation, identification and supply of synaptotagmin 2^{I377N} mice; these mice can be obtained from Ingenium Pharmaceuticals (michael.ade@ingenium-ag.com). We also thank Drs Weichun Lin and Yun Liu for help of electrophysiology for NMJs, Dr Rolf Joho for actometry and Han Dai for help with the CD experiments.

References

- Berton F, Iborra C, Boudier JA, Seagar MJ, Marqueze B (1997) Developmental regulation of synaptotagmin I, II, III, and IV mRNAs in the rat CNS. *J Neurosci* **17**: 1206–1216
- Borst JG, Helmchen F, Sakmann B (1995) Pre- and postsynaptic whole-cell recordings in the medial nucleus of the trapezoid body of the rat. *J Physiol* **489** (Part 3): 825–840
- Broadie K, Bellen HJ, DiAntonio A, Littleton JT, Schwarz TL (1994) Absence of synaptotagmin disrupts excitation–secretion coupling during synaptic transmission. *Proc Natl Acad Sci USA* **91**: 10727–10731
- DiAntonio A, Schwarz TL (1994) The effect on synaptic physiology of synaptotagmin mutations in *Drosophila*. *Neuron* **12**: 909–920
- Earles CA, Bai J, Wang P, Chapman ER (2001) The tandem C₂ domains of synaptotagmin contain redundant Ca²⁺ binding sites that cooperate to engage t-SNAREs and trigger exocytosis. *J Cell Biol* **154**: 1117–1123
- Fernandez I, Arac D, Ubach J, Gerber SH, Shin O, Gao Y, Anderson RG, Sudhof TC, Rizo J (2001) Three-dimensional structure of the synaptotagmin I C₂B-domain: synaptotagmin I as a phospholipid binding machine. *Neuron* **32**: 1057–1069
- Fernandez-Chacon R, Konigstorfer A, Gerber SH, Garcia J, Matos MF, Stevens CF, Brose N, Rizo J, Rosenmund C, Sudhof TC (2001) Synaptotagmin I functions as a calcium regulator of release probability. *Nature* **410**: 41–49
- Fowler SC, Birkestrand BR, Chen R, Moss SJ, Vorontsova E, Wang G, Zarcone TJ (2001) A force-plate actometer for quantitating rodent behaviors: illustrative data on locomotion, rotation, spatial patterning, stereotypies, and tremor. *J Neurosci Methods* **107**: 107–124
- Fukuda M, Aruga J, Niinobe M, Aimoto S, Mikoshiba K (1994) Inositol-1,3,4,5-tetrakisphosphate binding to C₂B domain of IP4BP/synaptotagmin II. *J Biol Chem* **269**: 29206–29211
- Geppert M, Archer III BT, Sudhof TC (1991) Synaptotagmin II. A novel differentially distributed form of synaptotagmin. *J Biol Chem* **266**: 13548–13552
- Geppert M, Goda Y, Hammer RE, Li C, Rosahl TW, Stevens CF, Sudhof TC (1994) Synaptotagmin I: a major Ca²⁺ sensor for transmitter release at a central synapse. *Cell* **79**: 717–727
- Guan KL, Dixon JE (1991) Eukaryotic proteins expressed in *Escherichia coli*: an improved thrombin cleavage and purification procedure of fusion proteins with glutathione S-transferase. *Anal Biochem* **192**: 262–267
- Hui E, Bai J, Wang P, Sugimori M, Llinas RR, Chapman ER (2005) Three distinct kinetic groupings of the synaptotagmin family: candidate sensors for rapid and delayed exocytosis. *Proc Natl Acad Sci USA* **102**: 5210–5214
- Li C, Davletov BA, Sudhof TC (1995a) Distinct Ca²⁺ and Sr²⁺ binding properties of synaptotagmins. Definition of candidate Ca²⁺ sensors for the fast and slow components of neurotransmitter release. *J Biol Chem* **270**: 24898–24902
- Li C, Ullrich B, Zhang JZ, Anderson RG, Brose N, Sudhof TC (1995b) Ca²⁺-dependent and -independent activities of neural and non-neural synaptotagmins. *Nature* **375**: 594–599
- Littleton JT, Stern M, Schulze K, Perin M, Bellen HJ (1993) Mutational analysis of *Drosophila* synaptotagmin demonstrates its essential role in Ca²⁺-activated neurotransmitter release. *Cell* **74**: 1125–1134
- Mackler JM, Drummond JA, Loewen CA, Robinson IM, Reist NE (2002) The C₂B Ca²⁺-binding motif of synaptotagmin is required for synaptic transmission *in vivo*. *Nature* **418**: 340–344
- Marek KW, Davis GW (2002) Transgenically encoded protein photo-inactivation (FlAsH-FALI): acute inactivation of synaptotagmin I. *Neuron* **36**: 805–813
- Marqueze B, Boudier JA, Mizuta M, Inagaki N, Seino S, Seagar M (1995) Cellular localization of synaptotagmin I, II, and III mRNAs in the central nervous system and pituitary and adrenal glands of the rat. *J Neurosci* **15**: 4906–4917
- Maximov A, Südhof TC (2005) Autonomous function of synaptotagmin I in triggering synchronous release independent of asynchronous release. *Neuron* **48**: 547–554
- McMahon HT, Missler M, Li C, Sudhof TC (1995) Complexins: cytosolic proteins that regulate SNAP receptor function. *Cell* **83**: 111–119
- Mehrotra B, Myszkowski DG, Prestwich GD (2000) Binding kinetics and ligand specificity for the interactions of the C₂B domain of synaptotagmin II with inositol polyphosphates and phosphoinositides. *Biochemistry* **39**: 9679–9686
- Morimoto T, Wang XH, Poo MM (1998) Overexpression of synaptotagmin modulates short-term synaptic plasticity at developing neuromuscular junctions. *Neuroscience* **82**: 969–978
- Nagy G, Kim JH, Pang ZP, Matti U, Rettig J, Sudhof TC, Sorensen JB (2006) Different effects on fast exocytosis induced by synaptotagmin 1 and 2 isoforms and abundance, but not by phosphorylation. *J Neurosci* **26**: 632–643
- Nishiki T, Augustine GJ (2004) Synaptotagmin I synchronizes transmitter release in mouse hippocampal neurons. *J Neurosci* **24**: 6127–6132
- Nonet ML, Grundahl K, Meyer BJ, Rand JB (1993) Synaptic function is impaired but not eliminated in *C. elegans* mutants lacking synaptotagmin. *Cell* **73**: 1291–1305
- Perin MS, Fried VA, Mignery GA, Jahn R, Südhof TC (1990) Phospholipid binding by a synaptic vesicle protein homologous to the regulatory region of protein kinase C. *Nature* **345**: 260–263
- Reim K, Mansour M, Varoqueaux F, McMahon HT, Südhof TC, Brose N, Rosenmund C (2001) Complexins regulate a late step in Ca²⁺-dependent neurotransmitter release. *Cell* **104**: 71–81
- Rickman C, Archer DA, Meunier FA, Craxton M, Fukuda M, Burgoyne RD, Davletov B (2004) Synaptotagmin interaction with the syntaxin/SNAP-25 dimer is mediated by an evolutionarily conserved motif and is sensitive to inositol hexakisphosphate. *J Biol Chem* **279**: 12574–12579
- Rosenmund C, Stevens CF (1996) Definition of the readily releasable pool of vesicles at hippocampal synapses. *Neuron* **16**: 1197–1207
- Russ A, Stumm G, Augustin M, Sedlmeier R, Wattler S, Nehls M (2002) Random mutagenesis in the mouse as a tool in drug discovery. *Drug Discov Today* **7**: 1175–1183
- Sakaba T, Neher E (2001) Quantitative relationship between transmitter release and calcium current at the calyx of held synapse. *J Neurosci* **21**: 462–476
- Shin OH, Rhee JS, Tang J, Sugita S, Rosenmund C, Südhof TC (2003) Sr²⁺ binding to the Ca²⁺ binding site of the synaptotagmin I C₂B domain triggers fast exocytosis without stimulating SNARE interactions. *Neuron* **37**: 99–108
- Shin OH, Rizo J, Südhof TC (2002) Synaptotagmin function in dense core vesicle exocytosis studied in cracked PC12 cells. *Nat Neurosci* **5**: 649–656
- Sommer I, Lingenhohl K, Friauf E (1993) Principal cells of the rat medial nucleus of the trapezoid body: an intracellular *in vivo* study of their physiology and morphology. *Exp Brain Res* **95**: 223–239
- Sorensen JB, Fernandez-Chacon R, Südhof TC, Neher E (2003) Examining synaptotagmin I function in dense core vesicle exocytosis under direct control of Ca²⁺. *J Gen Physiol* **122**: 265–276
- Stevens CF, Sullivan JM (2003) The synaptotagmin C₂A domain is part of the calcium sensor controlling fast synaptic transmission. *Neuron* **39**: 299–308
- Stumm G, Russ A, Nehls M (2002) Deductive genomics: a functional approach to identify innovative drug targets in the post-genome era. *Am J Pharmacogenomics* **2**: 263–271
- Sugita S, Han W, Butz S, Liu X, Fernandez-Chacon R, Lao Y, Südhof TC (2001) Synaptotagmin VII as a plasma membrane Ca²⁺ sensor in exocytosis. *Neuron* **30**: 459–473
- Sugita S, Shin OH, Han W, Lao Y, Südhof TC (2002) Synaptotagmins form a hierarchy of exocytotic Ca²⁺ sensors with distinct Ca²⁺ affinities. *EMBO J* **21**: 270–280
- Ubach J, Lao Y, Fernandez I, Arac D, Südhof TC, Rizo J (2001) The C₂B domain of synaptotagmin I is a Ca²⁺-binding module. *Biochemistry* **40**: 5854–5860
- Ubach J, Zhang X, Shao X, Südhof TC, Rizo J (1998) Ca²⁺ binding to synaptotagmin: how many Ca²⁺ ions bind to the tip of a C₂-domain? *EMBO J* **17**: 3921–3930
- Ullrich B, Li C, Zhang JZ, McMahon H, Anderson RG, Geppert M, Südhof TC (1994) Functional properties of multiple synaptotagmins in brain. *Neuron* **13**: 1281–1291
- Wu LG, Borst JG (1999) The reduced release probability of releasable vesicles during recovery from short-term synaptic depression. *Neuron* **23**: 821–832
- Yoshihara M, Littleton JT (2002) Synaptotagmin I functions as a calcium sensor to synchronize neurotransmitter release. *Neuron* **36**: 897–908
- Zhang X, Rizo J, Südhof TC (1998) Mechanism of phospholipid binding by the C₂A-domain of synaptotagmin I. *Biochemistry* **37**: 12395–12403